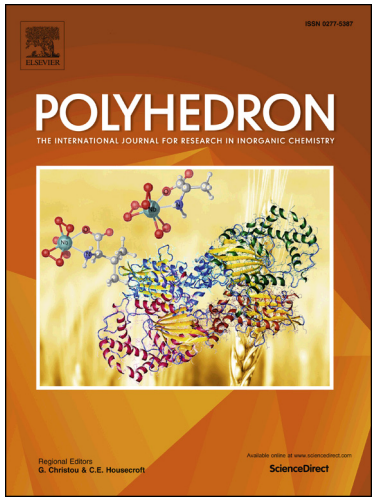

Cu(II), Ni(II) and Zn(II) mononuclear building blocks based on new polynucleating azomethine ligand: synthesis and characterization

Karolina Zdyb, Maxym O. Plutenko, Rostislav D. Lampeka, Matti Haukka, Malgorzata Ostrowska, Igor O. Fritsky, Elzbieta Gumienna-Kontecka

PII: S0277-5387(17)30492-8
DOI: http://dx.doi.org/10.1016/j.poly.2017.07.009
Reference: POLY 12745

To appear in: *Polyhedron*

Received Date: 10 May 2017
Accepted Date: 11 July 2017

Please cite this article as: K. Zdyb, M.O. Plutenko, R.D. Lampeka, M. Haukka, M. Ostrowska, I.O. Fritsky, E. Gumienna-Kontecka, Cu(II), Ni(II) and Zn(II) mononuclear building blocks based on new polynucleating azomethine ligand: synthesis and characterization, *Polyhedron* (2017), doi: http://dx.doi.org/10.1016/j.poly.2017.07.009

Cu(II), Ni(II) and Zn(II) mononuclear building blocks based on new polynucleating azomethine ligand: synthesis and characterization

Karolina Zdyb,[a] Maxym O. Plutenko,[b] Rostislav D. Lampeka,[b] Matti Haukka,[c] Malgorzata Ostrowska,[a] Igor O. Fritsky,[b] and Elzbieta Gumienna-Kontecka[a*]

[a] Faculty of Chemistry, University of Wrocław, F. Joliot-Curie 14, 50-383 Wrocław, Poland.

[b] Department of Chemistry, Taras Shevchenko National University of Kyiv, Volodymyrska 60, 01601 Kiev, Ukraine.

[c] Department of Chemistry, University of Jyväskylä, Seminaarinkatu 15 (C building), FI-40100 Jyväskylä, Finland

Five new mononuclear complexes formed by the polynucleating ligand 2-[1-(3,5-dimethyl)pyrazolyl]-2-hydroxyimino-N'-[1-(2-pyridyl)ethylidene]acetohydrazide (H**L**): [Ni(**L**)(H**L**)]ClO_4·2CH_3OH (**1**), [Ni(**L**)$_2$·CH_3OH (**2**), [Zn(**L**)(H**L**)]ClO_4·2CH_3OH (**3**), [Zn(**L**)$_2$]·CH_3OH (**4**) and [Cu(**L**)$_2$]·CH_3OH (**5**) were synthesized and characterized by elemental analysis, mass-spectrometry, IR- spectroscopy and X-ray analysis. The complexes reveal distorted octahedral N_4O_2 coordination arrangement formed by both protonated and deprotonated (**1**, **3**) or two deprotonated ligand molecules (**2**, **4**, **5**). The presence of non-coordinated oxime and pyrazole groups resulted in the formation of extensive systems of hydrogen bonds in the crystal packing of **1**-**5**. Potentiometric titrations, ESI-MS and spectrophotometric studies of complex formation in MeOH/H_2O solutions indicated the presence of mono- and polynuclear complexes with Cu(II), Ni(II) and Zn(II) ions. The solution studies carried out for an excess of Cu(II) over H**L** ligand (2:1 and 3:2 molar ratio) indicated also the formation of polynuclear $Cu_3L_2H_x$ species, with an involvement of additional nitrogen donors in copper coordination.In binuclear complex[$Cu_2(L)_2(DMF)_2$]$(ClO_4)_2$·DMF(**6**) obtained in solid state,the Cu(II) coordination, analogous to the one in **1**-**5**, was supported by pyrazole N atom.

Introduction

Polynucleating Schiff base ligands containing several various donor functions attract considerable attention because of their versatile, in some cases unpredictable, coordination properties and ability to form polynuclear metal complexes of various topologies.[1],[2] The presence of two or more different donor sets in the ligand molecule often allows obtaining polynuclear complexes with such original topologies as helicates,[3] metallacrowns[4] and molecular grids.[5-8]

Previously it was shown that polydentate Schiff base ligand H**pop** (Scheme 1) forms with transition metals ions polynuclear complexes with [2×2] molecular grid topology.[6] Particularly, two donor sets of H**pop** contain the donor atoms of different nature which promote the formation of the heterometalic grid-like [$Cu_2Mn_2(pop)_4(OAc)_4$] complex.[7] Although the preparation of molecular grids, in particular, heterometalic grids, are one-pot reactions, the formation of these complexes is likely a two-step self-assembly process.[6, 7] In the first step the mononuclear, metal-to-ligand 1:2species is formed. In the second step two such mononuclear bis-ligand species are aggregated with two additional transition metal ions to give the tetranuclear molecular grid. The implementation of these steps as separate synthetic stages expands synthetic abilities and can help to control the self-assembly processes.

The present work is devoted to the synthesis of new polydentate ligand 2-[1-(3,5-dimethyl)pyrazolyl]-2-hydroxyimino-N'-[1-(2-pyridyl)ethylidene]aceto-hydrazide (H**L**) (Scheme 1) containing several donor functions of different nature (*vide supra*), and the preparation of a series of complexes on its basis. Similarly to H**pop**, H**L** ligand possess two different donor sets, i.e. the pyridine plus azomethine (A) and oxime (B) having common amide O atom; also includes an additional donor set (C) formed by the pyrazole N and oxime O atoms.

The presence of three alternative donor compartments in **HL** makes the molecular design of the target polynuclear complexes complicated as any predictions on the topology and structure of the resulting metal complexes seem to be quite speculative and ambiguous. Moreover, the formation of a sole polynuclear species in this case could not be so straightforward as in the case of the ligands typically used for the preparation of molecular grids (like H**pop**) in which the number of donor atoms as a rule corresponds to the total number of positions available in the coordination spheres of all metal ions. Consequently, one-pot approach for polynuclear complexes can be complicated in the case of **HL** (see below) and thus seems to be unjustified. It is more reasonable and important to (i)define the primary donor sets in which metal binding occurs first, resulting in the formation of mononuclear species, and (ii) isolate the corresponding mononuclear complexes for further use as building blocks for the preparation of polynuclear assemblies. Thus, speciation studies in solution and isolation of mononuclear complexes (which a priori should contain vacant donor atoms or even donor compartments) should be regarded as a primary task in studies of donor properties of H**L**.

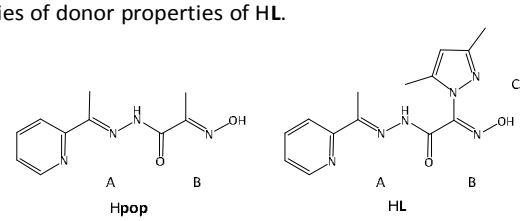

Scheme 1. Schematic depiction of H**pop** and H**L** ligands.

Material and methods

Materials

All of the reagents used in this work were of analytical grade and used without further purification. The solution studies were carried out in a MeOH/H_2O (80:20 w/w) mixture. The ionic strength was fixed at I = 0.1 M with $NaClO_4$. The solutions of Cu(II), Ni(II) and Zn(II) were prepared by dissolving $M(ClO_4)_2{\cdot}nH_2O$ (M = Cu(II), Ni(II) and Zn(II)) in water and standardized by ICP-AES. ***Caution!*** *Perchlorate salts combined with organic ligands are potentially explosive and should be handled in small quantity and with the necessary precautions.* $HClO_4$ solution was titrated by standardized NaOH in MeOH/H_2O solution. Carbonate-free NaOH solution was standardized by titration with potassium hydrogen phthalate.

Syntheses

Ethyl 2-[1-(3,5-dimethyl)pyrazolyl]-2-hydroxyiminoacetate: A mixture of ethyl 2-chloro-2-hydroxyiminoacetate (906 mg, 6 mmol, synthesized according to [9] and 3,5-dimethylpyrazol (1152 mg, 12 mmol) in 10 ml of chloroform was left for evaporation in the air overnight. The resulting solid residue was recrystallized from water. Yield: 1120 mg (88%). Found: C, 50.9; H, 6.4; N, 19.7. Calc. for $C_9H_{13}N_3O_3$: C, 51.18; H, 6.20; N, 19.89. ^{1}H-NMR (400 MHz, DMSO-d6, 25°C): 1.32 (3H, t, Et-CH_3, J=6.8), 2.10 (3H, s, Pz-CH_3), 2.15 (3H, s, Pz-CH_3), 4.27 (2H, quart., Et-CH_2, J=6.8), 5,89 (1H, s, Pz-CH), 12.92 (1H, s, oxime-OH).

2-[1-(3,5-dimethyl)pyrazolyl]-2-hydroxyiminoacetohydrazide: A solution of hydrazine hydrate in water (0.57 ml, 60%, 10.60 mmol) was added to a solution of ethyl 2-[1-(3,5-dimethyl)pyrazolyl]-2-hydroxyiminoacetate (1120 mg, 5.3 mmol) in methanol (30 ml). The resulting mixture was heated under reflux for 1.5 hours. After that the solvent was evaporated, and the solid residue was recrystallized from methanol. Yield 500 mg (48 %). Found: C, 42.8; H, 5.9; N, 35.3. Calc. for $C_7H_{11}N_5O_2$: C, 42.64; H, 5.62; N, 35.51. ^{1}H-NMR (400 MHz, DMSO-d_6, 25°C): 2.13 (3H, s, Pz-CH_3), 2.14 (3H, s, Pz-CH_3), 4.40 (2H, s, NH2), 5,87 (1H, s, Pz-CH), 9.56 (1H, s, NH), 12.23 (1H, s, oxime-OH). IR (KBr, cm-1): 1655 (νC=$O_{Amide\ I}$), 1022 (νN-O_{oxime}).

2-[1-(3,5-dimethyl)pyrazolyl]-2-hydroxyimino-N'-[1-(2-pyridyl)ethylidene]acetohydrazide (HL): A solution of 2-[1-(3,5-dimethyl)pyrazolyl]-2-hydroxyiminoacetohydrazide (500 mg, 2.54 mmol) in methanol (30 ml) was treated with 2-acetylpyridine (307 mg, 2.54 mmol) and the mixture was heated under reflux for 3 hours. After that the solvent was evaporated in vacuum and the crude product was recrystallized from methanol. Yield 650 mg (85%). Found: C, 55.9; H, 5.5; N, 27.8. Calc. for $C_{14}H_{16}N_6O_2$: C, 55.99; H, 5.37; N, 27.98. ^{1}H-NMR (400 MHz, DMSO-d_6, 25°C): 2.19 (6H, s, Pz-CH_3), 2.44 (3H, s, CH_3), 5.94 (1H, s, Pz-CH), 7.35 (1H, t, Py-5, J = 5.6 Hz), 7.79 (1H, t, Py-4, J = 7.6 Hz), 8.17 (1H, d, Py-3, J = 7.6 Hz), 8.56 (1H, d, Py-6, J = 5.6 Hz), 10.79 (1H, s, NH), 12.64 (1H, s, oxime-OH). IR (KBr, cm^{-1}): 1686 (νC=$O_{Amide\ I}$), 1045 (νN-O_{oxime}).

[Ni(L)(HL)]$ClO_4{\cdot}2CH_3OH$ (1): Solution of $Ni(ClO_4)_2{\cdot}6H_2O$ in methanol (0.1 M, 0.5 ml, 0.05 mmol) was added to solution of H**L** in methanol (0.1 M, 1 ml, 0.10 mmol). The resulting yellow-green mixture was stirred with heating for 40 min. Green single crystals suitable for X-ray analysis were grown by slow diffusion of vapors of diethyl ether into the diluted clear solution at room temperature (yield 21 mg, 51%). Found: C, 43.5; H, 4.9; N, 20.2. Calc. for $C_{30}H_{39}ClN_{12}O_{10}Ni$: C, 43.84; H, 4.78; N, 20.45. IR (KBr, cm^{-1}): 1622 (νC=$O_{Amide\ I}$), 1023 (νN-O_{oxime}).

[Ni(L)$_2$]·CH_3OH (2): Solution of NaOH in methanol (0.1 M, 1 ml, 0.10mmol) was added to solution of H**L** in methanol (0.1 M, 1 ml, 0.10mmol) and then solution of $Ni(ClO_4)_2{\cdot}6H_2O$ in methanol (0.1 M, 0.5 ml, 0.05 mmol) was added to the obtained mixture. The resulting yellow-green mixture was stirred with heating for 40 min, filtered off and left in air for crystallization. After one week green crystals of **2** suitable for X-ray analysis were obtained (yield 19 mg, 55 %). Found: C, 49.6; H, 4.8; N, 23.9. Calc. for $C_{29}H_{34}N_{12}O_5Zn$: C, 50.04; H, 4.92; N, 24.15. IR (KBr, cm^{-1}): 1624 (νC=$O_{Amide\ I}$), 1025 (νN-O_{oxime}).

[Zn(L)(HL)]$ClO_4{\cdot}2CH_3OH$ (3): Solution of $Zn(ClO_4)_2{\cdot}6H_2O$ in methanol (0.1 M, 0.5 ml, 0.05 mmol) was added to solution of H**L** in methanol (0.1 M, 1 ml, 0.10 mmol). The resulting yellow mixture was stirred with heating for 40 min, filtered off and left in air for crystallization. After one week yellow crystals of **3** suitable for X-ray analysis were obtained (yield 22 mg, 53%). Found: C, 43.2; H, 4.5; N, 20.0. Calc. for $C_{30}H_{39}ClN_{12}O_{10}Zn$: C, 43.49; H, 4.74; N, 20.29. ^{1}H-NMR (400 MHz, methanol-d_4, 25°C): 2.16 (3H, s, Pz-CH_3), 2.20 (3H, s, Pz-CH_3), 2.73 (3H, s, CH_3), 6.04 (1H, s, Pz-CH), 7.70 (1H, s, Py), 8.25 (2H, s, Py), 8.36 (1H, s, Py). IR (KBr, cm^{-1}): 1637 (νC=$O_{Amide\ I}$), 1021 (νN-O_{oxime}).

[Zn(L)$_2$]·CH_3OH (4): Solution of NaOH in methanol (0.1 M, 1 ml, 0.10mmol) was added to solution of H**L** in methanol (0.1 M, 1 ml, 0.10mmol) and then solution of $Zn(ClO_4)_2{\cdot}6H_2O$ in methanol (0.1 M, 0.5 ml, 0.05 mmol) was added to the obtained solution. The resulting yellow mixture was stirred with heating for 40 min, filtered off and left in air for crystallization. After one week yellow crystals of **4** suitable for X-ray analysis were obtained (yield 20mg, 58 %). Found: C, 49.6; H, 4.8; N, 23.9. Calc. for $C_{29}H_{34}N_{12}O_5Zn$: C, 50.04; H, 4.92; N, 24.15. ^{1}H-NMR (400 MHz, methanol-d_4, 25°C): 2.15 (3H, s, Pz-CH_3), 2.20 (3H, s, Pz-CH_3), 2.69 (3H, s, CH_3), 6.02 (1H, s, Pz-CH), 7.62 (1H, s, Py), 8.17 (2H, s, Py), 8.27 (1H, s, Py). IR (KBr, cm^{-1}): 1624 (νC=$O_{Amide\ I}$), 1025 (νN-O_{oxime}).

[Cu(L)$_2$]·CH_3OH (5): Solution of $Cu(ClO_4)_2{\cdot}6H_2O$ in methanol (0.1 M, 0.5 ml, 0.05 mmol) was added to solution of H**L** in methanol (0.1 M, 1 ml, 0.10mmol). The resulting yellow mixture was stirred with heating for 40 min, filtered off and left for crystallization in air. After one week yellow crystals of **5** suitable for X-ray analysis were obtained (yield 14 mg, 40%). Found: C, 49.7; H, 4.9; N, 23.8. Calc. for $C_{29}H_{34}N_{12}O_5Cu$: C, 50.17; H, 4.94; N, 24.21. IR (KBr, cm^{-1}): 1623 (νC=$O_{Amide\ I}$), 1025 (νN-O_{oxime}).

[Cu_2(L)$_2$(DMF)$_2$](ClO_4)$_2$·DMF (6): Solution of NaOH in methanol (0.1 M, 1 ml, 0.10mmol) was added to solution of H**L** in methanol (0.1 M, 1 ml, 0.10mmol) and then solution of $Cu(ClO_4)_2{\cdot}6H_2O$ in methanol (0.1 M, 1 ml, 0.10mmol) was added to the obtained solution. The resulting green-brown mixture was stirred with heating for 40 min, filtered off and left in air for methanol removing. Obtained brown amorphous remainder was dissolved in 5 ml of DMF. Green crystals suitable for X-ray analysis were obtained by slow diffusion of diethyl ether vapours into resulting DMF solution during one

month (yield 9 mg, 16%). IR (KBr, cm^{-1}): 1631 ($\nu C{=}O_{Amidel}$), 1025 ($\nu N{-}O_{oxime}$).

Physical measurements

Potentiometric titrations of H**L** and its complexes were performed using an automatic titrator system Titrando 905 (Metrohm) with a combined glass electrode (Mettler Toledo InLab Semi-Micro) calibrated daily in hydrogen ion concentration using $HClO_4$. The electrode was filled with 0.1M NaCl in MeOH/H_2O (80:20 w/w)ionic strength and conditioned two weeks before the first measurements were made. Between measurements electrode was stored in the same electrolyte solution. The experiments were carried out at 25±0.2°C and stream of Argon, pre-saturated with MeOH/H_2O(80:20 w/w) vapour, passed over the surface of the solution cell protecting from excessive evaporation of the sample. All the titrations were carried out on 3ml samples with the ligand concentration of $1\text{-}3\cdot10^{-3}$ M and metal to ligand molar ratios 1:1, 1:2,2:1 and 3:2 for Cu(II), 1:1 and 1:2 for Ni(II) and Zn(II). The exact concentration of the ligand was determined using the method of Gran.[10] The potentiometric data were refined with Superquad[11] program, which use nonlinear least-squares methods.[12]The obtained pKw in the solvent mixture used in measurements was -14.42.[13]

Absorption spectra were recorded using a Varian CARY 300 UV-Vis spectrophotometer at 25.0±0.2˚C. The spectrophotometric data were analyzed with SPECFIT[14] program. pH-dependent UV-Vis titrations were performed in the pH range 2-11. The combined glass electrode (Mettler Toledo InLab Semi-Micro) was prepared as in the case of potentiometric titration calibrated with buffers prepared in MeOH/H_2O (80:20 w/w) mixture before every measurement.[15] For Ni(II)-H**L** system, total volume of the solution containing 1:2 and 1:1 molar ratio of Ni(II):ligand was 7 ml. The concentration of the ligand was around $2\cdot10^{-3}$ M. The starting pH was adjusted to around 2 with $HClO_4$ and the titration was carried out in a cell with 5cm optical path length. For Cu(II), titrations were performed in a 1 cm cell with 3.2 ml as total volume of the solution containing 1:1, 1:2 and 2:1 molar ratios of Cu(II):ligand. The pH was controlled by addition of $HClO_4$.

EPR spectra were recorded on a Bruker ELEXSYS E500 CW-EPR spectrometer equipped with an NMR teslameter (ER 036TM) and frequency counter (E 41 FC) at X-band frequency, at 77K. The solutions for EPR were prepared by using MeOH/H_20 mixture (80/20 w/w). The experimental spectra were simulated using WINEPR Simfonia 1.26 program and Doubletnew (EPR OF S=1/2) program by Dr. Andrew Ozarowski, National High Field Magnetic Laboratory, University of Florida.

Electrospray ionization mass spectrometry (ESI-MS) data were collected in two series of experiments: (i) using a Jeol JMS-800D device or (ii) a Bruker apex ultra FT-ICR mass spectrometer and a BrukerMicrO-TOF-Q spectrometer (BrukerDaltonik, Germany), equipped with an Apollo II electrospray ionization source with an ion funnel. In the first series the 1-5 complexes were dissolved in methanol (concentration of 10^{-4}-10^{-6} M). For the second experiment stock solutions were prepared by using MeOH/H_2O mixture (80/20 w/w) as a solvent. The metal to ligand molar ratios were 1:1, 1:2 and 2:1 and the final pH of the solutions were 2 and 8. The instrument parameters were: dry gas–nitrogen, temperature 200°C, ion source voltage 4500 V, collision energy 10 eV. The instrument was calibrated using the Tunemix mixture (BrukerDaltonik, Germany) in the quadratic regression mode. During both experiments the spectra were recorded in the positive ion mode in the range 100 to 1500 m/z. The overall charge of the analyzed ion was calculated on the base of the distance between the isotopic peaks. For MS spectra analysis, a Bruker Compass DataAnalysis4.0 software was used.

^{1}H NMR spectra (400 MHz) were recorded using a Bruker AC-400 spectrometer at 293 K. IR spectra (KBr pellets) were recorded using a Perkin-Elmer Spectrum BX spectrometer in the wavenumber range 200-4000 cm^{-1} (Figure S1).

X-ray crystallography

All the measurements were performed using a NoniusKappa CCD diffractometer with a horizontally mounted graphite crystal as a monochromator and Mo Kα radiation. Data were collected and processed using Collect software.[16] The structures were solved and refined using the SHELXS-97 and SHELXL-97 programs, respectively.[17] For structure representation, the Diamond 3 program was used.[18]

Results and discussion

The H**L** ligand was synthesized from ethyl 2-chloro-2-hydroxyiminoacetate in three steps (Scheme 2).

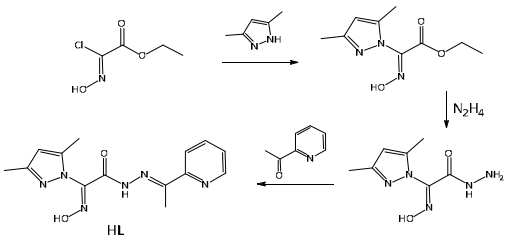

Scheme 2. Synthetic route to the H**L** ligand.

Compounds **1**-**5** were obtained by the reaction between the HL ligand and the corresponding metal salt in methanol, with or without an addition of alkali. It is important to note that the presence of metal ions facilitates the deprotonation of the amide group in such type of ligands.[6-8]Thus, the reaction of H**L** with zinc (II) and nickel (II) perchlorates gives complexes **1** and **3**, respectively, where one of two ligand molecules is deprotonated. The synthesis under the same experimental conditions, but performed with addition of one equivalent of sodium hydroxide, permits to obtain compounds **2** and **4**, where both ligand molecules are deprotonated. In the case of copper (II) perchlorate the deprotonation of both ligand molecules occurs without addition of alkali.

IR-spectroscopic studies of **1**-**5**show a limited low frequency shift of the ν(NO) band of the oxime group compared to the spectrum of H**L** (Δν = 20-24 cm^{-1} stretching mode), which suggests lack of involvement of this group in the coordination.[19] The long wave shift of the ν(CO) Amide I band of the amide group (Δν = 49-64 cm^{-1}) indicates the amide O atom coordination.[20, 21]

ESI-MS Spectrometry

Complex formation and the compositions of species formed in solution upon mixing H**L** ligand with Ni(II), Zn(II) and Cu(II)metal ions were first monitored using ESI-MS. Although this technique is not able to distinguish the ionizable protons in the species, the method can be successfully applied to determine the metal-to-ligand stoichiometry directly from the m/z values and has been successfully used by us when previously describing analogous systems.[6] Analysis of the ESI-MS spectra of the reaction mixture of Ni(II):H**L**, with a metal to ligand molar ratio 1:1, showed the formation of monomeric and oligomeric species successfully attributed to mononuclear $\{[NiL_2]+H^+\}^+$ (m/z 657.2), $\{[NiL_2]+Na^+\}^+$ (m/z 679.2), and polynuclear $\{[Ni_2L_3]^+\}^+$ (m/z 1013.2), $\{[Ni_2L_3]^+-H^++Na^+\}^+$ (m/z 1035.2), $\{[Ni_3L_3]^{3+}-2H^+\}^+$ (m/z 1071.2), $\{[Ni_4L_4]^{4+}-3H^+\}^+$ (m/z 1427.2) species (Figure 1). The recorded spectra were almost identical for solutions at pH of 2 and 8, as well as for Ni(II):H**L** 1:2 molar ratio. All peak assignments were based on the comparison between the calculated and experimental isotope patterns (Figure S2, Supplementary Material).

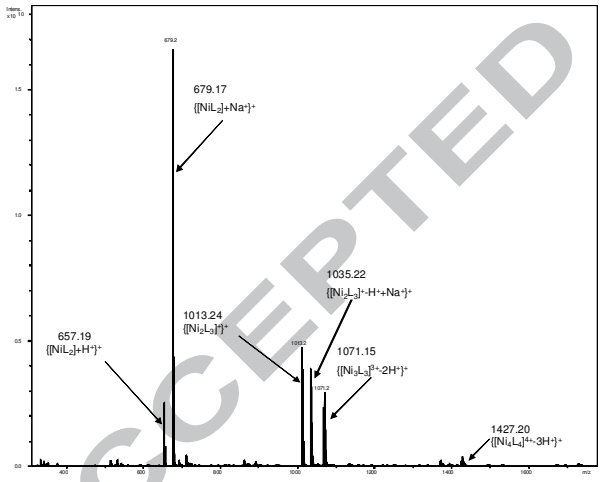

Figure. 1. ESI-MS spectra of the $Ni(ClO_4)_2$-H**L** system (pH 8) in methanol/water solution.

Similar behaviour has been observed for $Zn(ClO_4)_2$-H**L** system, where the following species were detected by ESI-MS: $\{[ZnL_2]+H^+\}^+$ (m/z 663.2), $\{[ZnL_2]+Na^+\}^+$ (m/z 685.2), $\{[ZnL_2]+K^+\}^+$ (m/z 701.1) and $\{[Zn_2L_3]^+\}^+$ (m/z 1029.2) (Figure S3).

The ESI-MS spectra of the reaction mixture of $Cu(ClO_4)_2$-H**L** were interpreted as: $\{[CuL]^+\}^+$ (m/z 362.1), $\{[CuL]^++H^++Cl^-\}^+$ (m/z 398.0), $\{[CuL]^++H^++ClO_4^-\}^+$ (m/z 462.0), $\{[CuL]^++ClO_4^-+Na^+\}^+$ (m/z 484.0), $\{[CuL_2]+H^+\}^+$ (m/z 662.0), $\{[Cu_2L_2]^{2+}-H^+\}^+$ (m/z 723.1), $\{[Cu_2L_2]^{2+}+ClO_4^-\}^+$ (m/z 825.1), $\{[Cu_2L_2]^{2+}-H^++Na^++ClO_4^-\}^+$ (m/z 847.0), $\{[Cu_2L_2]^{2+}+Na^++2ClO_4^-\}^+$, (m/z 947.0), $\{[Cu_2L_2]^{2+}-H^++2Na^++3ClO_4^-\}^+$ (m/z 1090.9) (Figure S5). The $\{[CuL]^++ClO_4^-+H^+\}^+$ species was predominating the solution.

Here again, the presence of $\{[CuL_2]+H^+\}^+$ was evidenced even at 1:1 metal to ligand molar ratio, and an excess of ligand in the solution gave spectra with the latter species predominating the solution. In the case of 2:1 metal to ligand molar ratio, at pH 3 only mononuclear $\{[CuL]^+\}^+$, $\{[CuL]^++H^++ClO_4^-\}^+$ and $\{[CuL]^++ClO_4^-+Na^+\}^+$ species were identified, however, at pH 9 the ESI-MS spectra showed the formation of oligomeric $\{[Cu_6L_4]^{8+}-6H^+\}^{2+}$ complex.

Methanolic solutions of the synthesized complexes **1**-**5** were also subjected to ESI-MS analysis. In the mass-spectra of all the complexes the patterns corresponding to mononuclear $\{[ML_2]+X^+\}^+$ species were found (M = Ni(II), Zn(II), Cu(II),X = H^+, Na^+ or K^+). Furthermore, low intensity signals (< 5%) corresponding to binuclear 2:3 species ($\{[Ni_2L_3]^+\}^+$, $\{[Ni_2L_3]^+-H^++Na^+\}^+$, $\{[Zn_2L_3]^+\}^+$, and $\{[Cu_2L_3]^+\}^+$) were also observed. The results of the mass-spectrometric experiments are collected in Table S1.

In spite of the fact that there is a low correlation between intensities of signals in ESI-MS mass-spectra and concentrations of corresponding species, we suppose that mononuclear complexes are prevailing in solution of all the systems studied in this work. At the same time binuclear species are probably minor species, which are formed from the mononuclear species due to the Equation 1.

$$2\{[ML_2] + X^+\}^+ \rightleftarrows \{[M_2(LH_{-1})L_2] + 2X^+\}^{2+} + HL \quad \textbf{Equation 1.}$$

(M = Ni(II), Zn(II) or Cu(II); $X^+ = H^+$, Na^+ or K^+)

The presence of such equilibrium suggests the possibility of the association of H**L**-containing mononuclear complexes into more complex supramolecular aggregates.

Speciation studies

Free ligand. In order to evaluate the coordination properties of the studied H**L** ligand toward metal ions, first the acid-base properties of this ligand were determined. The deprotonated form of the ligand, $[L]^-$, may attach three protons in the measured pH range, and the protonation constants determined are presented in Table 1. The first constant ($\log K_1$ = 8.77) corresponds to the protonation of oxime O^- group, the second ($\log K_2$ = 2.98) and the third ($\log K_3$ = 1.81) of the pyridine and pyrazole N atoms. The determination of microconstants and assignment of the successive protonation constants $\log K_2$ and $\log K_3$ to particular protonation site was not the goal of the work and was not studied in detail. Although slightly lower, $\log K_1$ and $\log K_2$ agree with the corresponding oxime and pyridine protonation constants determined for H**pop** ligand.[6] It should be emphasized that H**L** and H**pop** were measured under different experimental conditions ($MeOH/H_2O$ 80/20 w/w and $DMSO/H_2O$ 10/90 v/v, respectively), thereby precluding direct comparison of the data. However, the decrease of the protonation constants of H**L** ligand may come from an inductive effect of the pyrazole group.

Ni(II) and Zn(II) complexes. According to the potentiometric titrations, for Ni(II) and Zn(II) ions the stoichiometry of the complexes formed in solution were different for experiments performed in 1:1 and 1:2 metal to ligand molar ratios. In equimolar solutions only oligomeric species were found, starting from $[Ni_3\mathbf{L}_3H_2]^{2+}$ and $[Zn_3\mathbf{L}_3H_3]^{3+}$, for Ni(II) and Zn(II) respectively, up to $[M_3\mathbf{L}_3H_{-3}]^{3-}$, where M = Ni(II), Zn(II). For 1:2 metal-to-ligand molar ratio the speciation models obtained were best fitted with monomeric species, from $[Ni\mathbf{L}_2H]^{+}$/$[Zn\mathbf{L}_2H_2]^{2+}$ to $[M\mathbf{L}_2H_{-2}]^{2-}$ (Table 1, Figure 2).

In the spectrophotometric titration carried out for Ni(II)-H**L** in molar ratio 1:1 and 1:2, the d – d transitions centred at 864 nm (Table 1), present in the entire range of pH, suggest octahedral coordination of the Ni(II) ions (Figure S4).

Table 1. Potentiometric and spectroscopic data for proton and M(II) complexes of H**L**[a]

			UV-Vis	
species	log*β*	log *K*	λ (nm)	ε ($M^{-1}cm^{-1}$)
protonation of L				
H**L**	8.74 (2)	8.74		
$H_2\mathbf{L}$	11.72(4)	2.98		
$H_3\mathbf{L}$	13.53(6)	1.81		
Ni(II) complexes				
(Ni(II):L = 1:1)				
$[Ni_3H_2\mathbf{L}_3]^{5+}$	41.11(9)		864	11
$[Ni_3H\mathbf{L}_3]^{4+}$	38.03(7)	3.08	864	13
$[Ni_3\mathbf{L}_3]^{3+}$	33.4(1)	4.63	864	15
$[Ni_3\mathbf{L}_3H_{-1}]^{2+}$	27.8(1)	5.6	864	18
$[Ni_3\mathbf{L}_3H_{-2}]^{+}$	21.4(2)	6.4	864	21
$[Ni_3\mathbf{L}_3H_{-3}]$	12.1(1)	9.3	864	22
Ni(II) complexes				
(Ni(II):L = 1:2)				
$[NiH\mathbf{L}_2]^{+}$	22.25(3)		864	22
$[Ni\mathbf{L}_2]$	18.52(4)	3.73	864	39
$[Ni\mathbf{L}_2H_{-1}]^{-}$	8.33(5)	10.19	864	43
$[Ni\mathbf{L}_2H_{-2}]^{2-}$	-2.43(5)	10.76	864	45
Zn(II) complexes				
(Zn(II):L = 1:1)				
$[Zn_3H_3\mathbf{L}_3]^{6+}$	41.23(5)			
$[Zn_3H_2\mathbf{L}_3]^{5+}$	37.43(9)	3.80		
$[Zn_3H\mathbf{L}_3]^{4+}$	34.15(7)	3.28		
$[Zn_3\mathbf{L}_3]^{3+}$	27.39(5)	6.76		
$[Zn_3\mathbf{L}_3H_{-1}]^{2+}$	20.62(7)	6.77		
$[Zn_3\mathbf{L}_3H_{-2}]^{+}$	14.57(9)	6.05		
$[Zn_3\mathbf{L}_3H_{-3}]$	5.9(2)	8.67		
Zn(II) complexes				
(Zn(II):L = 1:2)				
$[ZnH_2\mathbf{L}_2]^{2+}$	23.79(3)			
$[ZnH\mathbf{L}_2]^{+}$	20.64(2)	3.15		
$[Zn\mathbf{L}_2]$	16.48(3)	4.16		
$[Zn\mathbf{L}_2H_{-1}]^{-}$	6.97(5)	9.51		
$[Zn\mathbf{L}_2H_{-2}]^{2-}$	-3.85(5)	10.82		

[a]Solvent: MeOH/H_2O 80:20 w/w, I= 0.1 M ($NaClO_4$), T = (25.0 ± 0.2) °C.

Cu(II) complexes. Calculations based on the potentiometric data obtained for equimolar solutions of Cu(II) and H**L** indicate the formation of monomeric and dimeric species, i.e. starting with $[Cu\mathbf{L}]^{+}$ predominating the solution in pH range 2-5.5, and followed by $[Cu_2\mathbf{L}_2H_{-1}]^{+}$ and $[Cu_2\mathbf{L}_2H_{-2}]$ (Table 2, Figure 3A). Using UV-Vis spectroscopy, we observed d-d transitions centred at 685 nm, which showed only small hypso- and hyperchromic shifts above pH 5.5 (Table 2, Figure S7). Such characteristics may indicate that in $[Cu\mathbf{L}]^{+}$ copper coordination is realized via two nitrogen donors, from the pyridine ring and from the azomethine group, and completed by an oxygen atom from amide group.

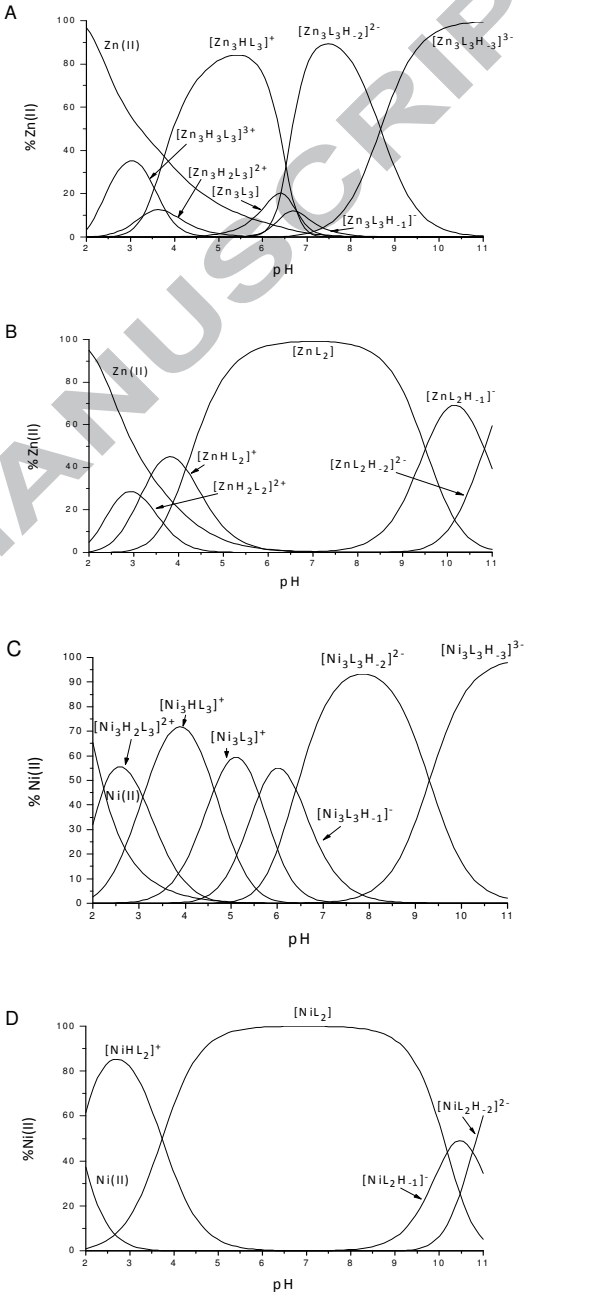

Figure 2. Species distribution profiles for Ni(II) and Zn(II) complexes of H**L**. A, C, E: M(II):H**L** in molar ratio M:H**L** = 1:1, B, D, F: M(II):H**L** in molar ratio M:H**L** = 1:2; [H**L**] = $2x10^{-3}$ M, I = 0.1 M ($NaClO_4$), MeOH/H_2O 80:20 w/w, T = (25.0 ± 0.2)°C.

In dimeric complexes an additional nitrogen atom from the pyrazole ring may support the copper binding (as observed in X-ray structure of **6**, Figure 7).Also EPR parameters strongly support the model based on monomeric and dimeric species (Figure S6). $[Cu\mathbf{L}]^+$ complex is characterized by A_{II} = 156.1 G and g_{II}= 2.25, while the spectra of dimeric species are distinguished

by the presence of three g factor values: g_x= 2.25, g_y= 2.12 and g_z= 2.03, what points toward the pentacoordination of Cu(II), and the geometry of the complex being intermediate between the square pyramid and the trigonal bipyramid (Figure7).[22] To distinguish between the two geometries, geometric parameters τ (Equation 2) and R (Equation 3) were calculated:

$$\tau = \frac{\beta - \alpha}{60} \qquad \textbf{Equation 2.}$$

where α is N(2)-Cu(1)-N(12) and N(6)-Cu(2)-N(8) angle and β is N(1)-Cu(1)-O(1) and N(7)-Cu(2)-O(3) angle for the first and the second Cu(II) ion, respectively;

$$R = \frac{g_y - g_z}{g_x - g_y} \qquad \textbf{Equation 3.}$$

g_x, g_y and g_z are g factor values of dimeric $[Cu_2\mathbf{L}_2H_{-x}]$ (x=1-6) species.[23]

The values of τ (τ_{Cu1}= 0.09, τ_{Cu2} = 0.05) and R (R = 0.64) parameters indicate the geometry of the distorted square pyramid with less than 10% share of the trigonal bipyramide.[23]

The potentiometric titrations performed for 1:2 Cu(II) to ligand molar ratio suggested the formation of the $[Cu\mathbf{L}]^+$ mononuclear species up to pH 5.5, followed by $[Cu\mathbf{L}_2]$, $[Cu\mathbf{L}_2H_{-1}]^-$ and $[Cu\mathbf{L}_2H_{-2}]^{2-}$ biscomplexes(Table 2, Figure 3B). The maximum of absorption spectra moves from 685 nm (ε = 110 $M^{-1}cm^{-1}$), through 574 (ε = 165 $M^{-1}cm^{-1}$), up to 554 nm (ε = 285 $M^{-1}cm^{-1}$) (Table 2, Figure S7), suggesting that Cu(II) changes the coordination environment from $\{N_{pyridine}, N_{azomethine}, O_{amide}\}$ to $2x\{N_{pyridine}, N_{azomethine}, O_{amide}\}$. The presence of mononuclear forms along the entire pH range studied (2-11) was confirmed by EPR spectra (Table 2). The EPR behaviour, i.e. a decrease of A_{II} from 153 G for $[Cu\mathbf{L}]^+$ till 114.5 G for $[Cu\mathbf{L}_2H_n]$ with almost constant g_{II} (Table 2, Figure S6) may be the result of a decrease in the symmetry of the complex. It has to be underlined that present speciation is different to the one previously observed for Cu(II):H**pop** system, where only biscomplexes were formed along the entire pH range.[6]

The solution studies carried out for an excess of Cu(II) over H**L** ligand (2:1 and 3:2 molar ratio) show that metal ion complexation again starts with the formation of the $[Cu\mathbf{L}]^+$ complex, and is followed by polynuclear $Cu_3\mathbf{L}_2H_x$ species (Table 2, Figure 3C).The distinct increase of the d–d transitions energy up to 630 nm indicate involvement of additional nitrogen donors in copper coordination (Figure S7). The disappearance of EPR signal confirms the formation of polynuclear species (Figure S6).

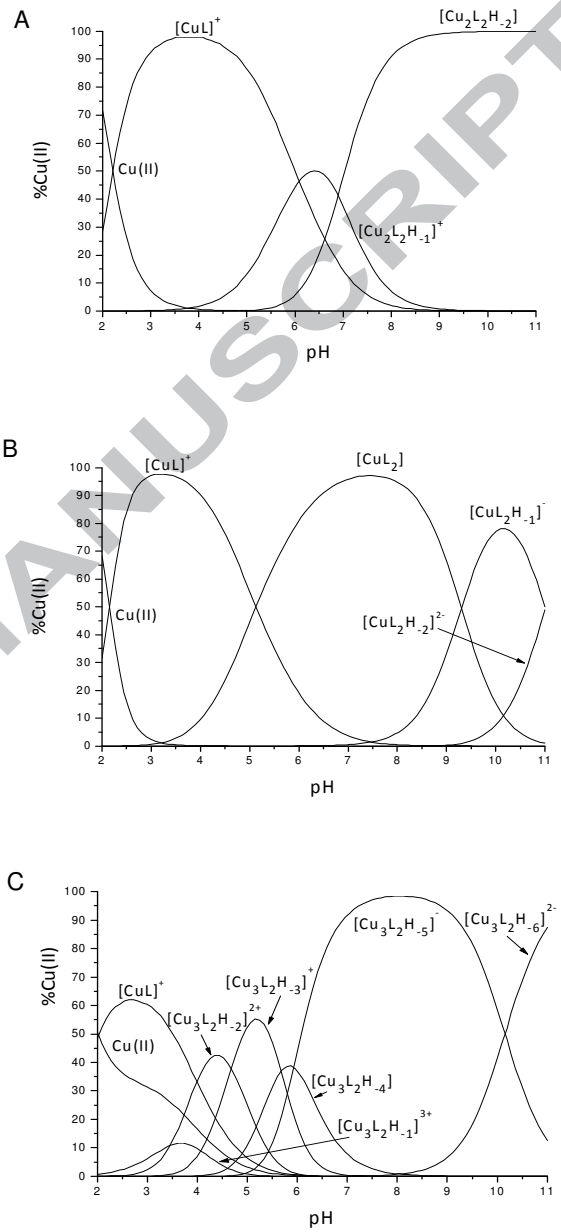

Figure 3. Species distribution profiles for Cu(II) complexes of H**L**. A: Cu(II)- H**L** in molar ratio M:H**L** = 1:1, B: Cu(II)- H**L** in molar ratio M:H**L** = 1:2, C: Cu(II)- H**L** in molar ratio M:H**L** = 2:1; [H**L**] = $2x10^{-3}$ M, I = 0.1 M ($NaClO_4$), MeOH/H_2O 80:20 w/w, T = (25.0 ± 0.2)°C.

Table 2. Potentiometric and spectroscopic data for Cu(II) complexes of H**L**[a]

			UV-Vis		EPR								
species	logβ	logK	λ (nm)	ε ($M^{-1}cm^{-1}$)	A_x	A_y	A_z	g_x	g_y	g_z	τ_{Cu1}	τ_{Cu2}	R
Cu(II):L = 1:1													
[Cu**L**]$^{+}$	10.74(2)		685	110	18	18	156.1	2.07	2.07	2.25			
[Cu$_2$**L**$_2$H$_{-1}$]$^{+}$	18.11(17)		660	245	108	35	30	2.25	2.12	2.03	0.09	0.05	0.64
[Cu$_2$**L**$_2$H$_{-2}$]	11.28(13)	6.83	668	400	108	35	30	2.25	2.12	2.03	0.09	0.05	0.64
Cu(II):L = 1:2													
[Cu**L**]$^{+}$	10.74(2)		685	110	18	18	156.1	2.07	2.07	2.25			
[Cu**L**$_2$]	17.62(8)		574	165	29	29	114.5	2.10	2.10	2.26			
[Cu**L**$_2$H$_{-1}$]$^{-}$	8.32(11)	9.30	554	285	29	29	114.5	2.10	2.10	2.26			
[Cu**L**$_2$H$_{-2}$]$^{2-}$	-2.69(13)	11.01	554	285	29	29	114.5	2.10	2.10	2.26			
Cu(II):L = 2:1													
[Cu**L**]$^{+}$	10.74(2)		685	110	18	18	156.1	2.07	2.07	2.25			
[Cu$_3$**L**$_2$H$_{-1}$]$^{3+}$	23.16(9)		630	160	EPR silent								
[Cu$_3$**L**$_2$H$_{-2}$]$^{2+}$	19.71(3)	3.45	630	160	EPR silent								
[Cu$_3$**L**$_2$H$_{-3}$]$^{+}$	15.03(5)	4.68	630	160	EPR silent								
[Cu$_3$**L**$_2$H$_{-4}$]	9.36(4)	5.67	630	160	EPR silent								
[Cu$_3$**L**$_2$H$_{-5}$]$^{-}$	3.43(7)	5.93	630	160	EPR silent								
[Cu$_3$**L**$_2$H$_{-6}$]$^{2-}$	-6.72(9)	10.15	630	160	EPR silent								

[a] Solvent: MeOH/H_2O 80:20 w/w, *I* = 0.1 M ($NaClO_4$), T = (25.0 ± 0.2) °C.

X-ray analysis

Mononuclear complexes. All the reported mononuclear complexes **1**-**5** are crystallized in P-1 space group with very close unit cell parameters (Table 3). The compounds **1** and **3** have similar ionic structures, which consist of the [M(**L**)(H**L**)]$^{+}$ (M = Ni(II) or Zn(II)) complex cation, perchlorate anion and two methanol solvent molecules (Figure 4). The perchlorate anion in structures **1** and **3** is disordered over two near positions; the distance between Cl atoms of two such positions is less than 0.7 Å. The compounds **2**, **4** and **5** have similar molecular structures, which consist of the neutral complex species [M(**L**)$_2$] (M = Cu(II), Ni(II) or Zn(II)) and methanol solvent molecules (Figure 4). Thus, compounds **1**-**5** reveal two structural types: molecular and ionic. The elements of crystal structures are connected by the extensive systems of hydrogen bonds. Selected bond lengths and angles are collected in Table 4.

The complex species [M(**L**)(H**L**)]$^{+}$ and [M(**L**)$_2$] include two ligand molecules and reveal similar structures. One or two ligand molecules are singly deprotonated in [M(**L**)(H**L**)]$^{+}$ and [M(**L**)$_2$], respectively. Note that the deprotonation occurs at the azomethine group, the amide nitrogen is deprotonated although it is not involved in the metal coordination. Such behaviour is similar to that observed in a series of H**pop**-containing complexes.[24-26] Both ligand molecules are coordinated in a tridentate {$N_{pyridine}$, $N_{azomethine}$, O_{amide}} mode, thus forming two fused five-membered chelate rings. The central atoms have the distorted octahedral coordination arrangements with N_4O_2 chromophores. Interestingly, in both complex species such an efficient donor as the oxime group remains uncoordinated and protonated, in spite of the fact that it can be involved in the chelate ring formation with the neighbouring pyrazole or amide nitrogen atoms. Presumably, the bis-chelating mode observed in **1** and **3** provides the most efficient donor set for primary metal binding.

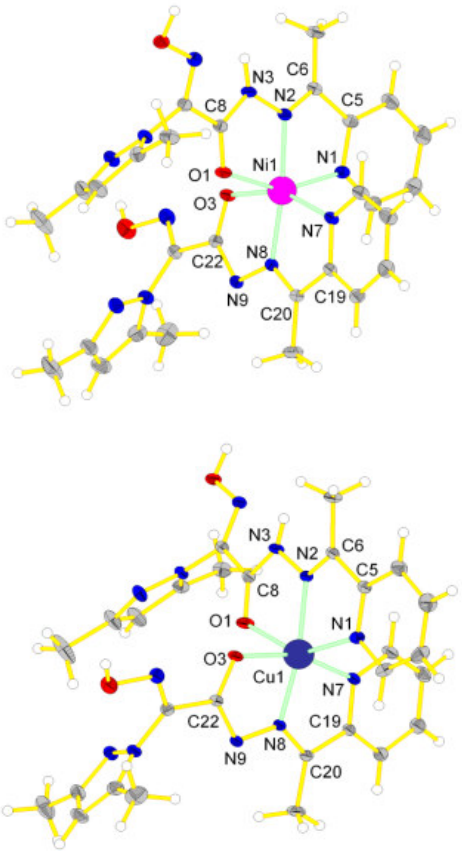

Figure 4. The structures of [Ni(**L**)(H**L**)]$^{+}$ complex cation of **1** (top) and [Cu(**L**)$_2$] of **5** (bottom).

Table 3. Crystallographic data for **1**-**5**.

Substance	**1**	**2**	**3**	**4**	**5**	**6**
Empirical formula	$C_{59}H_{74}Cl_2N_{24}$ Ni_2O_{19}	$C_{30}H_{41}ClN_{12}NiO_{11}$	$C_{59}H_{73}Cl_2N_{24}O_{19}Zn_2$	$C_{32}H_{46}N_{12}O_8Zn$	$C_{29}H_{35}CuN_{12}O_5$	$C_{37}H_{51}Cl_2Cu_2N_{15}O_{15}$
Formula weight	1611.70	839.91	1624.05	792.18	695.24	1143.91
Temperature (K)	100(2)	100(2)	150(2)	100(2)	100(2)	100(2)
Wavelength (Å)	0.71073	0.71073	0.71073	0.71073	0.71073	0.71073
Crystal system	Triclinic	Triclinic	Triclinic	Triclinic	Triclinic	Triclinic
Space group	P $\bar{1}$	P $\bar{1}$	P $\bar{1}$	P $\bar{1}$	P -1	P -1
Unit cell dimensions						
a (Å)	10.6303(3)	10.7043(2)	10.6569(3)	10.8509(3)	10.6915(3)	12.1309(3)
b (Å)	11.4519(3)	11.4389(2)	11.4695(3)	11.3171(3)	11.4517(3)	15.4364(4)
c (Å)	15.0083(4)	14.8083(3)	15.1619(4)	14.8271(4)	15.0562(4)	15.7753(6)
α (°)	77.7024(10)°	77.7370(10)	77.776(2)°	77.9980(10)°	77.444(2)°	111.885(2)°
β (°)	77.4310(10)°	76.9800(10)	76.735(2)°	76.2320(10)°	77.3300(10)°	110.855(2)°
γ(°)	81.7251(13)°	82.1410(10)	81.414(2)°	82.2400(10)°	81.8790(10)°	100.0050(10)°
Volume ($Å^3$)	1733.22(8)	1718.75(6)	1752.98(8)	1722.78(8)	1747.02(8)	2396.29(13)
Z	1	2	1	2	2	2
Density (calc) (Mg/m^3)	1.544	1.623	1.538	1.527	1.322	1.585
Absorptioncoefficient (mm^{-1})	0.710	0.723	0.849	0.784	0.679	1.081
F(000)	838	876	841	832	724	1180
Crystal size (mm^3)	0.41 x 0.15 x 0.07	0.38 x 0.22 x 0.13	0.47 x 0.17 x 0.06	0.38 x 0.22 x 0.13	0.31 x 0.20 x 0.12	0.41 x 0.31 x 0.07
Theta range for data collection	1.83 to 31.00°	1.83 to 33.30°	1.40 to 33.42°	1.85 to 33.38°	1.83 to 35.09°	1.57 to 33.25°
Index ranges	-15≤h≤15,-16≤k≤16, -21≤l≤21	-15≤h≤16,-17≤k≤17, 0≤l≤22	-16≤h≤16,-17≤k≤17, -23≤l≤23	-16≤h≤16,-16≤k≤17, 0≤l≤22	-16≤h≤17,-17≤k≤18, 0≤l≤24	-18≤h≤18,-23≤k≤23, -24≤l≤21
Reflections collected	40316	13062	34844	13236	15375	62467
Independent reflections	11019 (R_{int} = 0.0531)	13062 (R_{int} = 0.0000)	13540 (R_{int} = 0.0430)	13236	15375	18240 (R_{int} = 0.0227)
Absorption correction	Numerical	Semi-empirical from equivalents	Semi-empirical from equivalents	Semi-empirical from equivalents	Semi-empirical from equivalents	Semi-empirical from equivalents
Max. and min. transmission	0.9506 and 0.7571	0.9125 and 0.7718	0.9524 and 0.6890	0.9056 and 0.7560	0.9205 and 0.8196	0.9243 and 0.6686
Refinement method	Full-matrixleast-squareson F^2	Full-matrixleast-squareson F^2	Full-matrixleast-squareson F^2	Full-matrixleast-squareson F^2	Full-matrixleast-squareson F^2	Full-matrixleast-squareson F^2
Data / restraints / parameters	11019 / 115 / 492	13062 / 0 / 431	13540 / 13 / 522	13236 / 0 / 431	15375 / 0 / 432	18240 / 0 / 652
Goodness-of-fit on F^2	1.038	1.054	1.001	1.091	1.078	1.019
Final R indices [I>2sigma(I)]	R1 = 0.0451, wR2 = 0.1012	R1 = 0.0374, wR2 = 0.0911	R1 = 0.0492, wR2 = 0.0878	R1 = 0.0317, wR2 = 0.0875	R1 = 0.0443, wR2 = 0.1010	R1 = 0.0360, wR2 = 0.0952
R indices (all data)	R1 = 0.0733, wR2 = 0.1132	R1 = 0.0517, wR2 = 0.0946	R1 = 0.1114, wR2 = 0.1036	R1 = 0.0411, wR2 = 0.0909	R1 = 0.0677, wR2 = 0.1073	R1 = 0.0490, wR2 = 0.1030
Largest diff. peak and hole ($e.Å^{-3}$)	0.812 and -0.828	0.578 and -0.547	0.572 and -0.595	0.699 and -0.432	1.186 and -0.541	1.705 and -1.018

The Ni-N coordination bond lengths are ranging from 1.9822(15) to 2.0930(16) Å and 1.9911(9)-2.1034(10) Å, and Ni-O 2.0592(14)-2.1633(14) Å and 2.0780(9)-2.1302(9) Å in **1** and **2**,respectively. The Zn-N bond distances in **3** fall in the range 2.0592(14)-2.1592(15) Å, Zn-O 2.0924(13)-2.2511(13) Å, and in **4** the range of those distances is 2.0679(8)-2.1929(9) Å for Zn-N and 2.1130(7)-2.1480(8) Å for Zn-O.

Table 4. Selected bond lengths [Å] and angles [°] of **1**-**5**.

	1	**2**
Ni(1)-N(2)	2.0043(19)	1.9969(10)
Ni(1)-N(1)	2.0769(17)	2.0920(10)
Ni(1)-N(7)	2.0930(15)	2.1034(10)
Ni(1)-N(8)	1.9822(19)	1.9911(9)
Ni(1)-O(1)	2.1633(13)	2.1302(9)
Ni(1)-O(3)	2.0593(13)	2.0780(9)
O(1)-Ni(1)-N(2)	75.979(60)	76.44(4)
N(2)-Ni(1)-N(1)	77.645(66)	77.99(4)
N(7)-Ni(1)-N(8)	78.436(66)	78.23(4)
N(8)-Ni(1)-O(3)	77.530(62)	76.99(4)
	3	**4**
Zn(1)-N(2)	2.0950(1)	2.0679(0)
Zn(1)-N(1)	2.1270(1)	2.1929(0)
Zn(1)-N(7)	2.1592(1)	2.1841(0)
Zn(1)-N(8)	2.0592(0)	2.0866(0)
Zn(1)-O(1)	2.2511(1)	2.148(0)
Zn(1)-O(3)	2.0924(1)	2.113(0)
O(1)-Zn(1)-N(2)	72.861(1)	74.667(1)
N(2)-Zn(1)-N(1)	75.533(1)	75.366(1)
N(7)-Zn(1)-N(8)	76.387(1)	75.403(1)
N(8)-Zn(1)-O(3)	75.347(1)	74.404(1)
	5	
Cu(1)-N(2)	2.0576(10)	
Cu(1)-N(1)	2.2059(12)	
Cu(1)-N(7)	2.0480(11)	
Cu(1)-N(8)	1.9299(10)	
Cu(1)-O(1)	2.3844(10)	
Cu(1)-O(3)	2.0024(9)	
O(1)-Cu(1)-N(2)	72.69(4)	
N(2)-Cu(1)-N(1)	75.41(4)	
N(7)-Cu(1)-N(8)	79.99(4)	
N(8)-Cu(1)-O(3)	79.14(4)	

The Cu-N bond distances in **5** are in the range 1.9299(10)-2.2059(12) Å, Cu-O 2.0024(9)-2.3844(10)Å. The Zn-N and Zn-O bond lengths in the compounds **3** and **4** are comparable to the ones in previously reported zinc complexes with the pyridine and oxime groups complexed to the metal ion.[25, 27]

Bond angles O-M-O`, O-M-N, N-M-N` are typical for the pseudooctahedral coordination environment[28] (Table 2). The bite angles O(1)-M(1)-N(2), N(2)-M(1)-N(1), N(7)-M(1)-N(8) and N(8)-M(1)-O(3) are deviated from 90° (Table 4), which comes from the formation of five-membered chelate rings.The chelate rings M(1)O(1)C(8)N(3)N(2), M(1)N(2)C(6)C(5)N(1), M(1)N(7)C(19)C(20)N(8) and M(1)N(8)N(9)C(22)O(3) are almost planar.

Table 5. Hydrogen bond parameters of **1**-**5**.

D-H...A	d(D-H),Å	d(H...A),Å	d(D...A),Å	<(DHA),°
1				
O(2)-H(2O)...N(9)#1	0.92	1.81	2.714(2)	166.3
O(4)-H(4O)...O(9)#2	0.83	1.76	2.568(2)	163.4
O(9)-H(9O)...N(6)	0.88	1.89	2.776(3)	176.2
N(3)-H(3N)...O(10)	0.88	1.98	2.850(3)	170
2				
O(2)-H(2O)...N(9)#1	0.86	1.9	2.7522(13)	171.3
O(4)-H(4O)...O(5)	0.76	1.84	2.5763(15)	163.4
O(5)-H(5O)...N(6)#2	0.8	1.98	2.7622(15)	162.9
3				
O(2)-H(2O)...N(9)#1	0.82	1.89	2.7046(19)	171.6
O(4)-H(4O)...O(9)#2	0.88	1.77	2.602(2)	155.2
O(9)-H(9O)...N(6)	0.82	1.98	2.793(2)	168.8
N(3)-H(3N)...O(10)	0.86	2.03	2.881(3)	168.8
4				
O(2)-H(2O)...N(9)#1	0.87	1.9	2.7675(10)	173.3
O(4)-H(4O)...O(5)	0.76	1.86	2.5936(11)	163
O(5)-H(5O)...N(6)#2	0.8	2	2.7664(12)	161.5
5				
O(2)-H(2O)...N(9)#1	0.87	1.85	2.7126(13)	171.1
O(4)-H(4O)...O(5)	0.77	1.87	2.5837(15)	155.8
O(5)-H(5O)...N(6)#2	0.81	2	2.7679(16)	157.9

The deviations of the metal atoms from the mean plane formed by the other four atoms in the ring are less than 0.08Å. Bond lengths N-N', N-C and C-O of the azomethine group of H**L** are typical for the protonated moieties of these type (Table 4). At the same time the N-N', N-C and C-O bond lengths of **L** indicate values typical for the deprotonated azomethine group. The C=N and N-O bond lengths in the oxime moieties clearly indicate that the oxime groups exist in the nitroso rather than isonitroso form and are typical protonated oxime groups in the amide derivatives of 2-hydroxyiminopropanoic acid.[29]

In the $[M(\mathbf{L})(H\mathbf{L})]^+$ cation the azomethine oxygen atom is situated in an *anti*-position with respect to the oxime N atom in the case of H**L** and in *syn*-position in the case of **L**. There is a similar arrangement in of $[M(\mathbf{L})_2]$ molecule: one of the azomethine O atoms is situated in an *anti*-position with respect to the oxime N atom, another one - in *syn*-position. Note, that the free oxime group is normally located in *anti*-position to the amide group which was earlier shown in the structures of the free H**pop** ligand[30] and related amide derivatives of 2-hydroxyiminopropanoic acid[31].

The NC(=NOH)C(=O)NH fragments are not planar; the torsion angles O_{amide}-C-C-N_{oxime} are 159.6(2)° and 22.0(3)° for H**L** and **L** of **1** respectively, -161.1(0)° and -22.0(0)° for **2**, -159.0(1)° and -20.0(0)° for H**L** and **L** of **3** respectively, 157.9(0)° and -21.5(0)° for **4**, and -158.6(1)° and -20.2(2)° for **5**.
Hydrogen bond parameters of **1**-**5** are collected in Table 4.

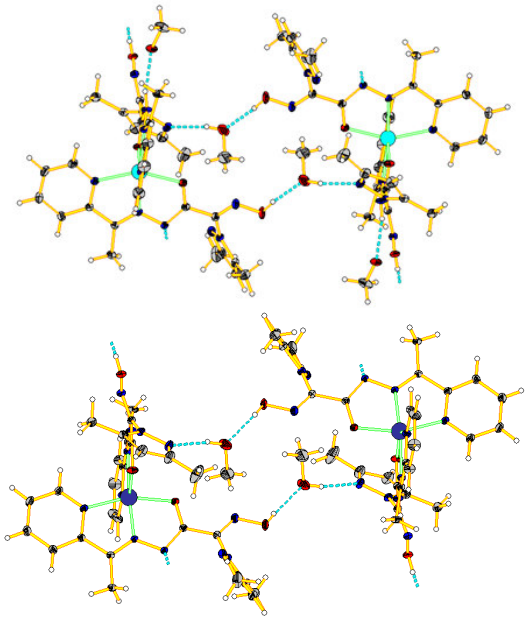

Figure 5. Fragments of crystal packing of **3** (top) and **5** (bottom).

There are two types of methanol molecules in the structures of **1** and **3**. The first type molecules form NH···O hydrogen bond where the amide N atom of H**L** acts as donor and the methanol molecule acts as acceptor. The molecules of the second type are involved in the formation of two hydrogen bonds: OH···O where the oxime O atom of **L** acts as donor and the methanol molecule acts as acceptor, and OH···N where the methanol molecule acts as donor and the pyrazole N atom of H**L** acts as receptor. Two $[M(\mathbf{L})(H\mathbf{L})]^+$ ions are connected through two methanol molecules of the second type by the system of hydrogen bonds, giving supramolecular unit like shown in Figure 5. In the crystal packing of **1** and **3** such units are connected by O-H···N hydrogen bonds into columns spreading along the *a* axis (Figure 6, scheme 3).

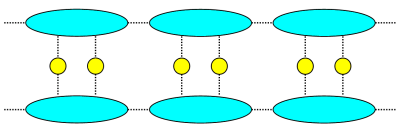

Scheme 3. Formation of columns along the a-axis in structures of **1**-**5**: ovals – $[M(\mathbf{L})(H\mathbf{L})]^+$ or $[M(\mathbf{L})_2]$, circles - methanol molecules, dot lines – hydrogen bonds.

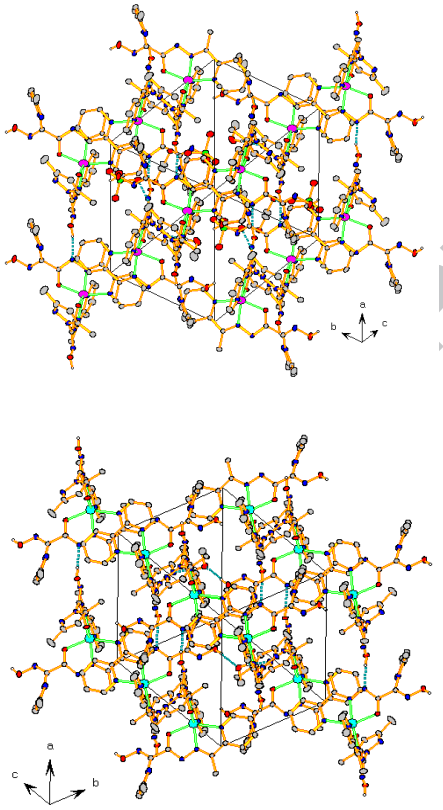

Figure 6. Crystal packing of **1** (top) and **4** (bottom).

The crystal packing of **2**, **4** and **5** is similar to the crystal packing of **1** and **3**. Two $[M(\mathbf{L})_2]$ molecules and two methanol molecules due hydrogen bonds form supramolecular units, which have similar structure to analogous units of **1** and **3** (Figure 5). These units are connected by O-H···N hydrogen bonds into columns spreading along the a-axis (Figure 6, Scheme 3).

Binuclear Cu(II) complex. The compound **6** is crystallized in P-1 space group and has ionic structure, which consists of the complex cation $[Cu_2(\mathbf{L})_2(DMF)_2]^{2+}$(Figure7), the perchlorate anion and two DMF solvent molecules. The elements of crystal structure are connected by the extensive systems of hydrogen bonds. Selected bond lengths and angles are collected in Table 6.

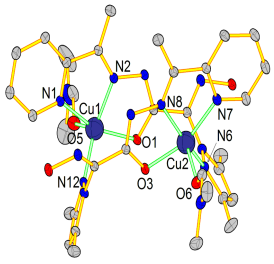

Figure 7. The structure of $[Cu_2(\mathbf{L})_2(DMF)_2]^{2+}$ (**6**) complex cation.

Both Cu(II) atoms of the complex cation $[Cu_2(\mathbf{L})_2(DMF)_2]^{2+}$ are equivalent and have distorted tetragonal-pyramidal N_3O_2 arrangement formed by the pyridine nitrogen atom, azomethine nitrogen atom and amide oxygen atom of the first ligand molecule, the pyrazole nitrogen atom of the second molecule of ligand, and the amide oxygen atom of the dimethylformamide molecule. Thus, both ligand molecules are coordinated in a tridentate-monodentate $\{(N_{pyrazole},N_{azomethine},O_{amide});(N'_{pyrazole})\}$-mode. Similarly to compounds **1**-**5**, the ligand molecules in $[Cu_2(\mathbf{L})_2(DMF)_2]^{2+}$ are singly deprotonated via the amide nitrogen atoms; the oxime groups are protonated and non-involved in coordination.

Table 6. Selected bond lengths [Å] and angles [°] of **6**.

Cu(1)-N(1)	2.0164(12)	Cu(2)-N(8)	1.9458(11)
Cu(1)-N(2)	1.9388(12)	Cu(2)-O(3)	1.9865(10)
Cu(1)-N(12)	1.9640(12)	Cu(2)-O(6)	2.1472(11)
Cu(1)-O(1)	2.0001(10)	N(2)-Cu(1)-N(1)	80.35(5)
Cu(1)-O(5)	2.1418(12)	N(2)-Cu(1)-O(1)	98.00(5)
Cu(2)-N(6)	1.9806(11)	N(8)-Cu(2)-N(7)	80.38(5)
Cu(2)-N(7)	2.0009(13)	N(8)-Cu(2)-O(3)	79.73(5)

The Cu-N bond distances in **6** are in the range 1.9388(12)-2.0164(12) Å, Cu-O – 1.9865(10)-2.1472(11) Å, what is typical for tetragonal-pyramidal complexes of copper with similar ligands.[23] The distance between the two copper atoms is 4.50(1) Å. Bond angles O-M-O`, O-M-N, N-M-N` have typical values for the tetragonal-pyramidal arrangement (Table 6). The bite angles N(2)-Cu(1)-N(1), N(2)-Cu(1)-O(1), N(8)-Cu(2)-N(7) and N(8)-Cu(2)-O(3) are deviated from the value of 90° (Table 6), which is conditioned by the formation of five-membered chelate rings.

The chelate rings Cu(1)N(1)C(6)C(5)N(2),Cu(1)N(2)N(2)C(8)O(1), Cu(2)N(7)C(19)C(20)N(8) and Cu(2)N(8)N(9)C(22)O(3) are almost planar. The deviations of the metal atoms from the mean plane formed by the other four atoms in the rings are less than 0.1 Å.

Bond lengths N-N', N-C and C-O have typical values for the deprotonated azomethine group (Table 6). The C=N and N-O bond lengths are typical for the non-coordinated non-deprotonated oxime groups in the nitroso form.[22-26]

In both ligand molecules of $[Cu_2(\mathbf{L})_2(DMF)_2]^{2+}$ the azomethine oxygen atom is situated in an anti-position with respect to the oxime N atom. The NC(=NOH)C(=O)NH fragments are not planar; the torsion angles O_{amide}-C-C-N_{oxime} are 154.8(1)° and 156.9(1)°.

Hydrogen bond parameters of **6** are collected in Table 7.

Table 7. Hydrogen bond parameters of **6**.

D-H...A	d(D-H), Å	d(H...A), Å	d(D...A), Å	<(DHA), °
O(2)-H(2O)...N(3)#1	0.81	1.98	2.765(2)	163.7
O(4)-H(4O)...N(9)#2	0.87	1.91	2.753(2)	162.2

Each complex cation $[Cu_2(\mathbf{L})_2(DMF)_2]^{2+}$is connected with two neighbouring cations through two hydrogen bonds, in which the oxime O atom acts as donor and the amide N atom acts as acceptor. Due to these hydrogen bonds in the crystal packing of **6**(Figure 8) the columns spreading along the ac diagonal are formed.

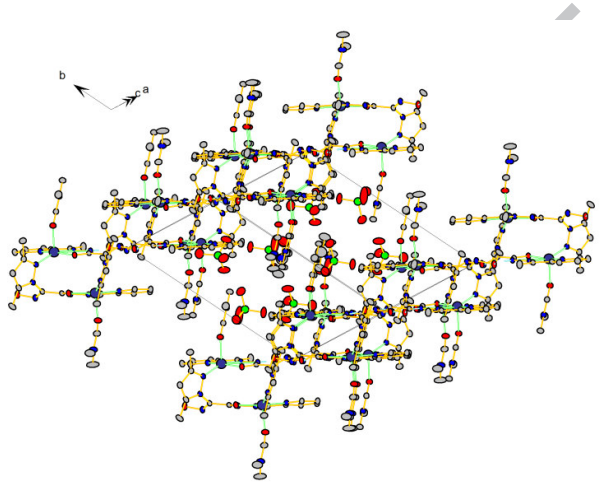

Figure 8. Crystal packing of **6**.

Conclusions

A new polynucleating azomethine ligand H**L** has been successfully used with Ni(II), Cu(II) and Zn(II) salts to obtain a series of mononuclear and binuclear complexes, characterized both in solution and solid state.

Solution studies of H**L** ligand demonstrate its ability to form stable complexes with a stoichiometry dependent on the metal to ligand molar ratio applied in the experiment. In the case of equimolar solutions the formation of oligomeric species was observed for Ni(II) and Zn(II) ions, however, for the Cu(II) complexation led to the formation of dimeric complexes. The two-fold molecular stoichiometry of the ligand vs metal ion promoted formation of monomeric $[M\mathbf{L}_2H_x]$ complexes, where M = Ni(II), Zn(II), Cu(II). In 2:1 and 3:2 Cu(II) to ligand molar ratios the complexation occurs with the formation of the polynuclear $Cu_3\mathbf{L}_2H_x$ species, preceded by the creation of $[Cu\mathbf{L}]^+$ complex.

In a series of mononuclear complexes **1**-**5**obtained in solid state the corresponding metal ion has a distorted octahedral coordination arrangement N_4O_2 formed by two ligand molecules. H**L** molecules are coordinated in the protonated or the singly deprotonated form via the pyridine and the azomethine nitrogen atoms and the amide oxygen atom. Such coordination mode is typical for mononuclear complexes based on already described polynucleating azomethine ligand H**pop**: Zn[**pop**]$_2$·2H_2O and Zn[(H**pop**)Cl_2]·2H_2O[21, 24]. It is important to note that the reaction of H**pop** with $ZnCl_2$ proceeds without ligand deprotonation giving Zn[(H**pop**)Cl_2]·2H_2O[24], but at the same time in the structures of **1**-**5** half of ligand molecules are deprotonated. Thus, the

amide group of H**L** is, most probably, more inclined to the deprotonation than analogous group of H**pop**. It can be explained by lower electron density on the amide group of H**L** because of the presence of electron-deficient pyrazole ring in the ligand molecule.

In **1**-**5** compounds only one of three donor sets of the ligand is involved in coordination to the metal ion. Thus, there are four vacant donor atoms in the reported complexes which are available for coordination of extra metal ions. Moreover, these donor atoms can form two adjacent bidentate chelating units, i.e. $\{N_{amide}, N_{oxime}\}$ and $\{O_{oxime}, N_{pyrazole}\}$. Therefore **1**-**5** can be regarded as promising building blocks for obtaining of coordination compounds of higher nuclearity. It is partially proved by the results of ESI mass-spectrometry which suggest the presence of binuclear species in $M(ClO_4)_2$-H**L**(M = Ni(II), Zn(II), Cu(II)) solutions with a metal to ligand molar ratio 1:1. Moreover, $Ni(ClO_4)_2$-H**L**solution reveal the formation of trinuclear $\{[Ni_3\mathbf{L}_3]^{3+}\text{-}2H^+\}^+$ and tetranuclear $\{[Ni_4\mathbf{L}_4]^{4+}\text{-}3H^+\}^+$ species. In the case of 2:1 Cu(II) to ligand molar ratio at pH 9 the hexanuclear complex $\{[Cu_6\mathbf{L}_4]^{8+}\text{-}6H^+\}^{2+}$ formation was observed. $\{[M_2\mathbf{L}H_{-1}\mathbf{L}_2]^+ + X^+\}^{2+}$ (X^+ = H^+, Na^+, K^+) binuclear species is observed in methanol solution of **1**-**5**, thereby suggesting the possibility of associative assembly of such complexes.

In binuclear complex **6** obtained in solid state both Cu(II) atoms are equivalent and have distorted tetragonal-pyramidal N_3O_2 arrangement formed by two ligand molecules and molecule of DMF. Both ligand molecules are singly deprotonated and coordinated in a tridentate-monodentate {(N,N',O);(N'')}-mode. The coordination mode is similar to the one in **1**-**5** but it additionally includes coordinated pyrazole N atom.

The involvement of H**L**-containing mononuclear complexes by metal ions into more complex coordination compounds is more predictable and controlled process than the direct reactions between the ligand and metal salts in a certain metal-to-ligand ratio. Presently synthetic work aimed in preparation and characterization of such polynuclear compounds is underway in our laboratories.

Appendix A. Supplementary data

CCDC 1534659–1534664 contains the supplementary crystallographic data for **1**-**6** complexes. These data can be obtained free of charge via http://www.ccdc.cam.ac.uk/conts/retrieving.html, or from the Cambridge Crystallographic Data Centre, 12 Union Road, Cambridge CB2 1EZ, UK; fax: (+44) 1223-336-033; or e-mail: deposit@ccdc.cam.ac.uk.

Acknowledgements

The financial support from the Polish National Science Centre (2015/19/B/ST5/00413), the State Fund for Fundamental Researches of Ukraine (grant No. F40.3/041) and the Swedish Institute (Visby Program) is gratefully acknowledged.

Notes and references

[1] L. Zhao, V. Niel, L. K. Thompson, Z. Q. Xu, V. A. Milway, R. G. Harvey, D. O. Miller, C. Wilson, M. Leech, J. A. K. Howard, S. L. Heath, *Dalton Transactions* **2004**, 1446-1455; M. U. Anwar, K. V. Shuvaev, L. N. Dawe, L. K. Thompson, *Inorganic Chemistry* **2011**, *50*, 12141-12154.

[2] P. A. Vigato, S. Tamburini, *Coordination Chemistry Reviews* **2004**, *248*, 1717-2128.

[3] S. Naskar, M. Corbella, A. J. Blake, S. K. Chattopadhyay, *Dalton Transactions* **2007**, 1150-1159; M. R. Bermejo, A. M. Gonzalez-Noya, M. Martinez-Calvo, R. Pedrido, M. J. Romero, M. V. Lopez, *European Journal of Inorganic Chemistry* **2008**, 3852-3863.

[4] G. Mezei, C. M. Zaleski, V. L. Pecoraro, *Chemical Reviews* **2007**, *107*, 4933-5003; Y. Bai, D. B. Dang, C. Y. Duan, Y. Song, Q. J. Meng, *Inorganic Chemistry* **2005**, *44*, 5972-5974.

[5] M. Ruben, J. Rojo, F. J. Romero-Salguero, L. H. Uppadine, J. M. Lehn, *Angewandte Chemie-International Edition* **2004**, *43*, 3644-3662.

[6] Y. S. Moroz, K. Kulon, M. Haukka, E. Gumienna-Kontecka, H. Kozlowski, F. Meyer, I. O. Fritsky, *Inorganic Chemistry* **2008**, *47*, 5656-5665.

[7] Y. S. Moroz, L. Szyrwiel, S. Demeshko, H. Kozlowski, F. Meyer, I. O. Fritsky, *Inorganic Chemistry* **2010**, *49*, 4750-4752.

[8] Y. S. Moroz, S. Demeshko, M. Haukka, A. Mokhir, U. Mitra, M. Stocker, P. Mueller, F. Meyer, I. O. Fritsky, *Inorganic Chemistry* **2012**, *51*, 7445-7447.

[9] A. P. Kozikowski, M. Adamczyk, *Journal of Organic Chemistry* **1983**, *48*, 366-372.

[10] G. Gran, *Acta Chemica Scandinavica* **1950**, *4*, 559-577.

[11] P. Gans, A. Sabatini, A. Vacca, *Journal of the Chemical Society-Dalton Transactions* **1985**, 1195-1200.

[12] G. Peter, *Data Fitting in the Chemical Sciences*, John Wiley & Sons, **1992**.

[13] W. J. Mackellar, D. B. Rorabacher, *Journal of the American Chemical Society* **1971**, *93*, 4379-+.

[14] F. J. Rossotti, H. S. Rossotti, R. J. Whewell, *Journal of Inorganic & Nuclear Chemistry* **1971**, *33*, 2051-&; H. Gampp, M. Maeder, C. J. Meyer, A. D. Zuberbuehler, *Analytica Chimica Acta* **1987**, *193*, 287-293; H. Gampp, M. Maeder, C. J. Meyer, A. D. Zuberbuhler, *Talanta* **1986**, *33*, 943-951.

[15] C. L. Deligny, P. F. M. Luykx, M. Rehbach, A. A. Wieneke, *Recueil Des Travaux Chimiques Des Pays-Bas-Journal of the Royal Netherlands Chemical Society* **1960**, *79*, 699-712; C. L. Deligny, P. F. M. Luykx, M. Rehbach, A. A. Wieneke, *Recueil Des Travaux Chimiques Des Pays-Bas-Journal of the Royal Netherlands Chemical Society* **1960**, *79*, 713-726.

[16] Hooft, R. W. W., COLLECT, Bruker AXS BV, Delft, The Netherlands, **2004**

[17] Sheldrick, G.M., SHELXS97 and SHELXL97. Program for Crystal Structure Solution and Refinement. University of Göttingen, Göttingen, **1997**;Sheldrick, G. M., Acta Cryst. **2015**, C71, 3-8.

[18] H. Putz and K. Brandenburg, Diamond - Crystal and Molecular Structure Visualization, Crystal Impact GbR, Bonn, Germany, **2004**.

[19] M. E. Keeney, K. Osseoasare, K. A. Woode, *Coordination Chemistry Reviews* **1984**, *59*, 141-201; A. M. Duda, A. Karaczyn, H. Kozlowski, I. O. Fritsky, T. Glowiak, E. V. Prisyazhnaya, T. Y. Sliva, J. SwiatekKozlowska, *Journal of the Chemical Society-Dalton Transactions* **1997**, 3853-3859; T. Y. Sliva, T. KowalikJankowska, V. M. Amirkhanov, T. Glowiak, C. O. Onindo, I. O. Fritsky, H. Kozlowski, *Journal of Inorganic Biochemistry* **1997**, *65*, 287-294; C. O. Onindo, T. Y. Silva, T. Kowalikjankowska, I. O. Fritsky, P. Buglyo, L. D. Pettit, H. Kozlowski, T. Kiss, *Journal of the Chemical Society-Dalton Transactions* **1995**, 3911-3915.

[20] V. V. Skopenko, R. D. Lampeka, I. O. Fritskii, *Doklady Akademii Nauk Sssr* **1990**, *312*, 123-128; I. O. Fritsky, H. Kozlowski, P. J. Sadler, O. P. Yefetova, J. Swatek-Kozlowska, V. A. Kalibabchuk, T. Glowiak, *Journal of the Chemical Society-Dalton Transactions* **1998**, 3269-3274.

[21] I. O. Fritsky, J. Swiatek-Kozlowska, A. Dobosz, T. Y. Sliva, N. M. Dudarenko, *Inorganica Chimica Acta* **2004**, *357*, 3746-3752.

[22] A. I. Buvailo, E. Gumienna-Kontecka, S. V. Pavlova, I. O. Fritsky, M. Haukka, *Dalton Transactions* **2010**, *39*, 6266-6275; E. Garribba, G. Micera, *Journal of Chemical Education* **2006**, *83*, 1229-1232.

[23] A. ADDISON, T. RAO, J. REEDIJK, J. VANRIJN, G. VERSCHOOR, *Journal of the Chemical Society-Dalton Transactions* **1984**, 1349-1356.

[24] Y. S. Moroz, K. O. Znovjyak, I. O. Golenya, S. V. Pavlova, M. Haukka, *Acta Crystallographica Section E-Structure Reports Online* **2010**, *66*, M242-U1449.

[25] Y. S. Moroz, T. Y. Sliva, K. Kulon, H. Kozlowski, I. O. Fritsky, *Acta Crystallographica Section E-Structure Reports Online* **2008**, *64*, M353-U727.

[26] A. Kufelnicki, S. V. Tomyn, Y. S. Moroz, M. Haukka, J. Jaciubek-Rosinska, I. O. Fritsky, *Polyhedron* **2012**, *33*, 410-416.

[27] S. R. Petrusenko, V. N. Kokozay, I. O. Fritsky, *Polyhedron* **1997**, *16*, 267-274; L. V. Penkova, A. Maciag, E. V. Rybak-Akimova, M. Haukka, V. A. Pavlenko, T. S. Iskenderov, H. Kozlowski, F. Meyer, I. O. Fritsky, *Inorganic Chemistry* **2009**, *48*, 6960-6971.

[28] S. Konar, A. Jana, K. Das, S. Ray, S. Chatterjee, J. A. Golen, A. L. Rheingold, S. K. Kar, *Polyhedron* **2011**, *30*, 2801-2808; P. Sathyadevi, P. Krishnamoorthy, E. Jayanthi, R. R. Butorac, A. H. Cowley, N. Dharmaraj, *Inorganica Chimica Acta* **2012**, *384*, 83-96; L. V. Ababei, A. Kriza, C. Andronescu, A. M. Musuc, *Journal of Thermal Analysis and Calorimetry* **2012**, *107*, 573-584.

[29] O. M. Kanderal, H. Kozlowski, A. Dobosz, J. Swiatek-Kozlowska, F. Meyer, I. O. Fritsky, *Dalton Transactions* **2005**, 1428-1437; I. O. Fritsky, H. Kozlowski, O. M. Kanderal, M. Haukka, J. Swiatek-Kozlowska, E. Gumienna-Kontecka, F. Meyer, *Chemical Communications* **2006**, 4125-4127; A. Dobosz, N. M. Dudarenko, I. O. Fritsky, T. Glowiak, A. Karaczyn, H. Kozlowski, T. Y. Silva, J. Swiatek-Kozlowska, *Journal of the Chemical Society-Dalton Transactions* **1999**, 743-749; A. A. Mokhir, E. Gumienna-Kontecka, J. Swiatek-Kozlowska, E. G. Petkova, I. O. Fritsky, L. Jerzykiewicz, A. A. Kapshuk, T. Y. Sliva, *Inorganica Chimica Acta* **2002**, *329*, 113-121.

[30] Y. S. Moroz, V. A. Kalibabchuk, E. Gumienna-Kontecka, V. V. Skopenko, S. V. Pavlova, *Acta Crystallographica Section E-Structure Reports Online* **2009**, *65*, O2413-+.

[31] R. D. Lampeka, A. A. Dvorkin, Y. A. Simonov, I. O. Fritsky, V. V. Skopenko, *Ukrainskii Khimicheskii Zhurnal* **1989**, *55*, 458-461; A. A. Dvorkin, I. A. Simonov, V. V. Skopenko, I. O. Fritskii, R. D. Lampeka, *Doklady Akademii Nauk Sssr* **1990**, *313*, 98-101; A. A. Dvorkin, I. O. Fritskii, I. A. Simonov, R. D. Lampeka, M. D. Mazus, T. I. Malinovskii, *Doklady Akademii Nauk Sssr* **1990**, *310*, 87-90.

Graphical abstract

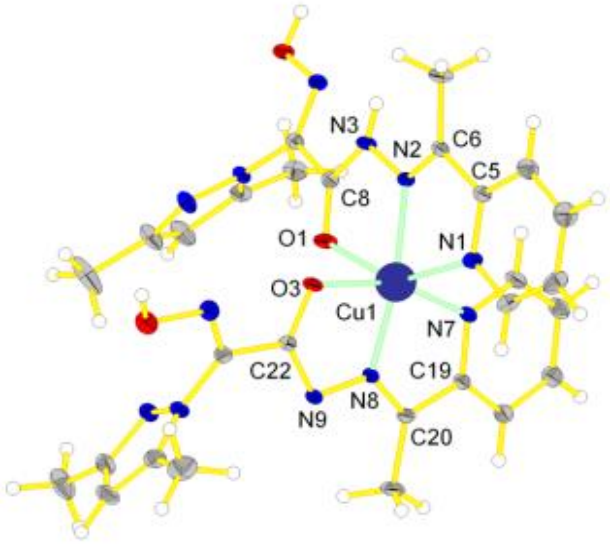

The new polynucleating ligand possessing several donor functions of different nature (pyridine, azomethine, oxime and pyrazole groups) have been synthesized. A series of complexes on its basis have been characterized in solution and solid state as a preliminary studies to preparation and characterization of more complex coordination compounds.